CONF-74-135-E
E-0125

E 125

Submitted to the
17th International Conference
on High-Energy Physics
London, 1-10 July 1974

CERN/D.Ph.II/PHYS 74-27
28.6.1974

# PRODUCTION OF $K^o_s$, $\Lambda$ AND $\gamma$ IN 100 GeV/c $\pi^- p$ INTERACTIONS

E.L. Berger*, V.T. Cocconi, M.J. Counihan**, S. Humble***,
G. Kellner, A. Kotanski+, D. Kuhn++, S.B. Ljung+++,
D.R.O. Morrison, P. Schmid°, R. Stroynowski, F.A. Triantis and H. Wahl

CERN, Geneva

ABSTRACT

Results are presented on the production of $K^o_s$, $\Lambda$ and $\gamma$ in 100 GeV/c $\pi^- p$ interactions in the 30-inch hydrogen bubble chamber at NAL. The cross sections for the production of $\pi^o$, $K^o_s$, $\Lambda$ and $\bar{\Lambda}$ are derived and compared with those produced in other reactions as functions of the energy. The average number of $\pi^o$ produced per collision is the same as in 100 GeV/c pp reactions.

* Visiting Scientist from Argonne National Laboratory.

** CERN Fellow from Imperial College, London.

*** Visiting Scientist from the Daresbury Laboratory.

+ Visiting Scientist from the Jagellonian University, Cracow.

++ CERN Fellow from Physikalisches Institut der Universität, Innsbruck.

+++ Visiting Scientist from Helsinki University.

° CERN Fellow from Institut für Hochenergiephysik, Vienna.

DROM/ef

CERN/D.Ph.II//PHYS 74-27

## 1. INTRODUCTION

Preliminary results are presented for inclusive $\gamma$, $K_S^O$ and $\Lambda$ production in $\pi^-p$ interactions at 100 GeV/c. The data come from a 50 000 picture exposure of the 30" hydrogen bubble chamber at the Fermi National Accelerator Laboratory. About 10 400 events were found after scanning the film twice. All events were pre-measured and then measured automatically on the CERN HPD. Some 37% of the events were remeasured.

The measurement results were processed through the standard CERN geometry and kinematics reconstruction programs.

This paper is based on 633 $V^O$'s, representing about 40% of the final sample of $V^O$'s.

About 20% of these $V^O$'s failed the kinematical reconstruction. For the others, cuts were made in the reconstructed effective mass squared of the $V^O$'s, the distance from the primary vertex and the average transverse momentum of the $V^O$-decay products with respect to the line of flight of the $V^O$.

The final sample after cuts consists of 223 $\gamma$'s, 102 $K_S^O$, 60 $\Lambda$ and 4 $\bar{\Lambda}$. Additional 26 ambiguous $V^O$'s were classified with equal weight among the non-ambiguous hypotheses.

Corrections were made for neutral decay modes, for conversion and decay outside the chamber [1], for the failed events and for the cuts applied.

The resulting average weights for the $\gamma$, $K^O$ and $\Lambda$'s are 67.4, 2.79, and 2.86, respectively.

## 2. CROSS SECTIONS

The $\pi^-p$ total cross section at 100 GeV/c found in this experiment is 24.1 ± 0.5 mb, obtained from scanning statistics for events and for beam tracks in the bubble chamber. This is consistent with the value of 23.96 ± 0.14 recently given by Carrol et al. [2].

The cross sections for inclusive $\gamma$, $K_S^O$, $\Lambda$ and $\bar{\Lambda}$ production are 118.2 ± 7.8, 2.43 ± 0.23, 1.6 ± 0.20 and 0.22 ± 0.05 mb, respectively. Assuming

that all $\gamma$'s observed come from $\pi^o$'s, the inclusive $\pi^o$ production cross section is 59.1 ± 3.9 mb. These cross sections are compared in figs. 1-4 with values reported at other energies for different incident particles [3-5].

In fig. 1 it may be seen that the $\pi^o$ production cross section, $\sigma(\pi^o)$, in $\pi^-p$ reactions is always below that for pp reactions and the ratio of these $\sigma(\pi^o)$ is approximately equal to the ratio of $\pi^-p$ to pp total inelastic cross sections.

The $K_s^o$ productions cross section, $\sigma(K_s^o)$, shown in fig. 2 is higher for $\pi^-p$ than for pp collisions at low energies (<∿30 GeV/c), because of threshold effects. At 100 GeV/c, however, $\sigma(K_s^o)$ for $\pi^-p$ collisions is below that for pp, the ratio again being approximately the ratio of their respective total inelastic cross sections.

In fig. 3, $\sigma(\Lambda)$ for $\pi^-p$ is comparable with that for pp at low energies, where threshold effects are important, but falls below the pp values at 100 GeV/c, being approximately half. This ratio could be considered to be the ratio of their respective total inelastic cross sections but it may be more correct to consider it as being a reflection of the fact that there is only one initial baryon in $\pi^-p$ collisions and two in pp collisions (it may be noted that anti-lambda production is very small, and hence the lambdas produced are almost entirely from the fragmentation of the initial baryons and not from baryon-antibaryon production).

In fig. 4 is shown the cross sections for the production of anti-lambdas in $\pi^{\pm}p$, $K^{\pm}p$, and pp reactions. There is an overall trend for the cross sections to rise sharply with increasing energy. For comparison the curve for the production of antiprotons in pp collisions [6] is given and it may be seen to exhibit a similar behaviour.

The average numbers of $\pi^o$, $K_s^o$ and $\Lambda$'s per inelastic interaction are given in table 1 and are compared in figs. 5 and 6 with values at other energies and for various incident particles. The average number of $\pi^o$'s is the same in pp and $\pi^-p$ collisions in our energy range, whereas the average number of $K_s^o$ and $\Lambda$'s is slightly lower than in pp collisions. In table 1 and in fig. 7 we present also the average number of $\pi^o$, $K_s^o$ and $\Lambda$'s per

inelastic collision of a given charged multiplicity; (the charged multiplicity cross sections are from ref. 7). The straight line in fig. 7a is obtained using the formula of ref. 8, and it is seen to approximate the experimental points satisfactorily (the decrease at the highest multiplicities is caused by phase space effects). The average numbers of $K_s^o$ and $\Lambda$'s are essentially independent of the charged multiplicity.

## 3. INCLUSIVE DISTRIBUTIONS

Fig. 8 shows the integral over $p_t^2$ of the invariant cross section

$$f(x, p_t^2) = \frac{2E}{\pi\sqrt{s}} \frac{d^2\sigma}{d\,x\,d\,p_t^2} \qquad \text{for } \gamma,\ K_s^o \text{ and } \Lambda.$$

Results are given only in the backward hemisphere in the centre of mass, since experimental losses for $K_s^o$ and $\Lambda$ are less severe here than in the forward hemisphere.

The results for $\gamma$ and $K_s^o$ indicate an exponential decrease as $|x|$ increases; the shape of the $\Lambda$ distribution suggests that the $\Lambda$'s come predominantly from proton fragmentation. The integral of $f(x, p_t^2)$ over x is shown in fig. 9.

Fig. 10 gives the rapidity distributions. The distribution for gammas is presented here also in the forward hemisphere, and it can be seen that over two units of rapidity around $y \approx 0$ the distribution is in first approximation flat. No such plateau is seen in the $K_s^o$ distributions.

We are deeply indebted to the operating crews of the Fermi NAL accelerator and of the 30-inch bubble chamber. We would like to thank our scanning, measuring and computing staffs.

REFERENCES

[1] T.M. Knasel, DESY Reports 70/2 and 70/3 (1970), unpublished.

[2] A.S. Carrol et al., "Total Cross Sections of $\pi^{\pm}$, $K^{\pm}$, p and $\bar{p}$ on protons and deuterons between 50 and 200 GeV/c".
Contribution to 18th Int. Conference on High Energy Physics, London, July 1974.

[3] NAL data from:

J.W. Chapman et al., "Production of $\gamma$, $\Lambda^{o}$, $K_{s}^{o}$ and $\bar{\Lambda}$ in pp Collisions at 102 GeV/c", Univ. of Rochester Report No. UR 457 (1973).

G. Charlton et al., Phys. Rev. Letters 29 (1972) 1759 and Phys. Rev. Letters 30 (1973) 1192.

F.T. Dao et al., Phys. Rev. Letters 30 (1973) 1151.

D. Bogert et al., Contribution to Berkeley Meeting APS/DPF (1973).

J.W. Chapman et al., Contribution to Berkeley Meeting APS/DPF (1973).

[4] Serpukhov data from:

H. Blumenfeld et al., Physics Letters 45B (1973) 525 and Physics Letters 45B (1973) 528.

"Inclusive Production of $\Lambda^{o}$, $K^{n}$ and $\gamma$ in $K^{-}p$ interactions at 32 GeV/c", France-Soviet Union and CERN-Soviet Union Collaborations, Contribution to 2nd Int. Conference in Aix-en-Provence, 1973.

"Production of $\gamma$ Rays in $K^{\pm}p$ Interactions at 32 GeV/c", France-Soviet Union and CERN-Soviet Union Collaborations, Contribution to this Conference.

"Neutral K, $\Lambda$ and $\bar{\Lambda}$ Production in $K^{\pm}p$ Interactions at 32 GeV/c", France-Soviet Union and CERN-Soviet Union Collaborations, Contribution to this Conference.

[5] J. Whitmore, "Experimental Results on Strong Interactions in the NAL Hydrogen Bubble Chamber", NAL-Pub-73/70-EXP, (1973) and references therein for lower energy data.

[6] M. Antinucci et al., Lettere al Nuovo Cimento 6 (1973) 121.

[7] "Multiplicity cross sections for 100 GeV/c $\pi^- p$ Interactions", E.L. Berger et al., CERN/D.Ph.II/PHYS 74-9.

[8] P. Grassberger and H.I. Miettinen, "On the Charge Structure of High Energy Multiple Production", CERN preprint TH. 1870 (1974).

TABLE 1

Average number of $\pi^o$, $K_s^o$ and $\Lambda$'s per inelastic collision and production cross sections for individual charged multiplicities in $\pi^- p$ collisions at 100 GeV/c *)

| Prong Number n | $\langle n_{\pi^o} \rangle_n$ | $\sigma_n(\pi^o)$ (mb) | $\langle n_{K_s^o} \rangle_n$ | $\sigma_n(K_s^o)$ (mb) | $\langle n_\Lambda \rangle_n$ | $\sigma_n(\Lambda)$ (mb) |
|---|---|---|---|---|---|---|
| 0 | — | — | 0.5 ± 0.6 | 0.02 ± 0.02 | 0.61 ± 0.7 | 0.02 ± 0.02 |
| 2 | 1.3 ± 0.4 | 2.5 ± 0.8 | 0.12 ± 0.04 | 0.23 ± 0.08 | 0.05 ± 0.03 | 0.10 ± 0.05 |
| 4 | 2.3 ± 0.4 | 11.0 ± 1.7 | 0.09 ± 0.02 | 0.43 ± 0.09 | 0.10 ± 0.02 | 0.48 ± 0.10 |
| 6 | 2.5 ± 0.4 | 12.9 ± 1.8 | 0.13 ± 0.02 | 0.67 ± 0.12 | 0.07 ± 0.02 | 0.36 ± 0.09 |
| 8 | 3.9 ± 0.5 | 16.8 ± 2.2 | 0.12 ± 0.03 | 0.52 ± 0.10 | 0.07 ± 0.02 | 0.30 ± 0.08 |
| 10 | 3.4 ± 0.6 | 8.5 ± 1.5 | 0.14 ± 0.04 | 0.35 ± 0.19 | 0.06 ± 0.02 | 0.15 ± 0.06 |
| 12 | 3.4 ± 0.9 | 4.8 ± 1.3 | 0.07 ± 0.03 | 0.10 ± 0.05 | 0.13 ± 0.05 | 0.18 ± 0.08 |
| 14 | 3.9 ± 1.6 | 2.3 ± 1.0 | 0.11 ± 0.08 | 0.07 ± 0.05 | 0.03 ± 0.06 | 0.02 ± 0.04 |
| 16 | 1.1 ± 1.4 | 0.15 ± 0.2 | 0.12 ± 0.15 | 0.016 ± 0.02 | — | — |
| ALL MULT. | 2.84 ± 0.19 | 59.1 ± 3.9 | 0.116 ± 0.012 | 2.43 ± 0.23 | 0.077 ± 0.009 | 1.61 ± 0.20 |

*) Errors are statistical only.

CERN/D.Ph.II/PHYS 74-27

FIGURE CAPTIONS

1. Cross sections for $\pi^o$ production as functions of incident momentum for various types of incident particles [3 - 5].

2. As fig. 1 for $K_s^o$ production.

3. As fig. 1 for $\Lambda$ production.

4. As fig. 1 for $\bar{\Lambda}$ production.

5. Average number of $\pi^o$'s produced per inelastic collision for $\pi^{\pm}p$, pp, $\pi^-n$ and $K^{\pm}p$ interactions [5].

6. Average number of $K_s^o$ and $\Lambda$'s produced per inelastic collision in $\pi^-p$ and pp reactions [3 - 5].

7. Average number of a) $\pi^o$, b) $K_s^o$, and c) $\Lambda$'s per inelastic collision as a function of the negative particle mulitiplicity. The straight line in fig. 7a is obtained using a formula from ref. [8].

8. Invariant cross section integrated over $p_t^2$, as a function of x for inclusive production of a) $\gamma$, b) $K_s^o$ and c) $\Lambda$ in $\pi^-p$ collisions at 100 GeV/c.

9. Invariant cross section integrated over x, as a function of $p_t^2$, for inclusive production of a) $\gamma$, b) $K_s^o$ and c) $\Lambda$ in $\pi^-p$ collisions at 100 GeV/c.

10. Invariant cross section integrated over $p_t^2$, as a function of center of mass rapidity y, for inclusive production of a) $\gamma$, b) $K_s^o$ and c) $\Lambda$ in $\pi^-p$ collisions at 100 GeV/c.

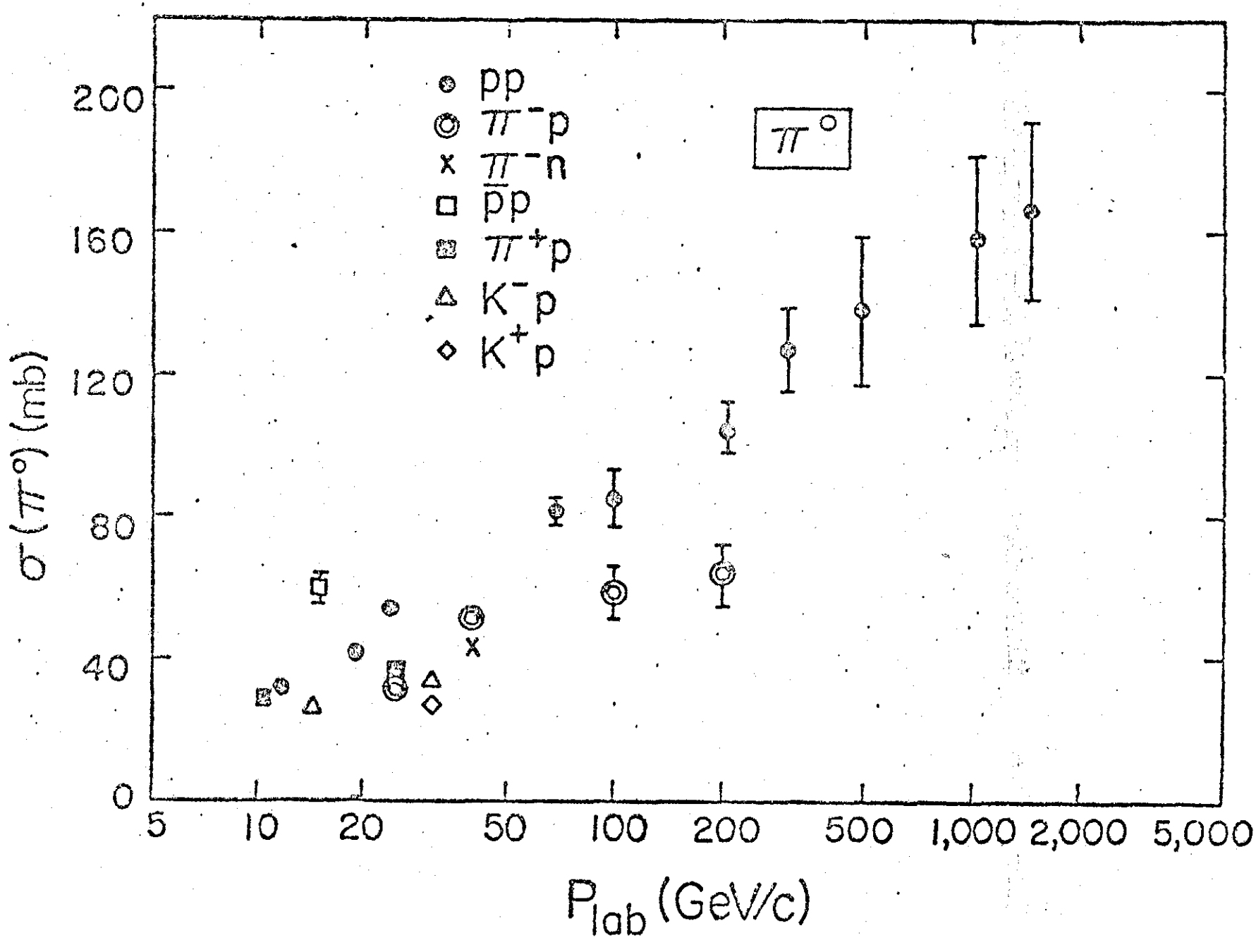
pp
π⁻p
π⁻n
p̄p
π⁺p
K⁻p
K⁺p
π°
σ(π°) (mb)
0
40
80
120
160
200
5
10
20
50
100
200
500
1,000
2,000
5,000
P_lab (GeV/c)

Fig. 1

Fig. 2

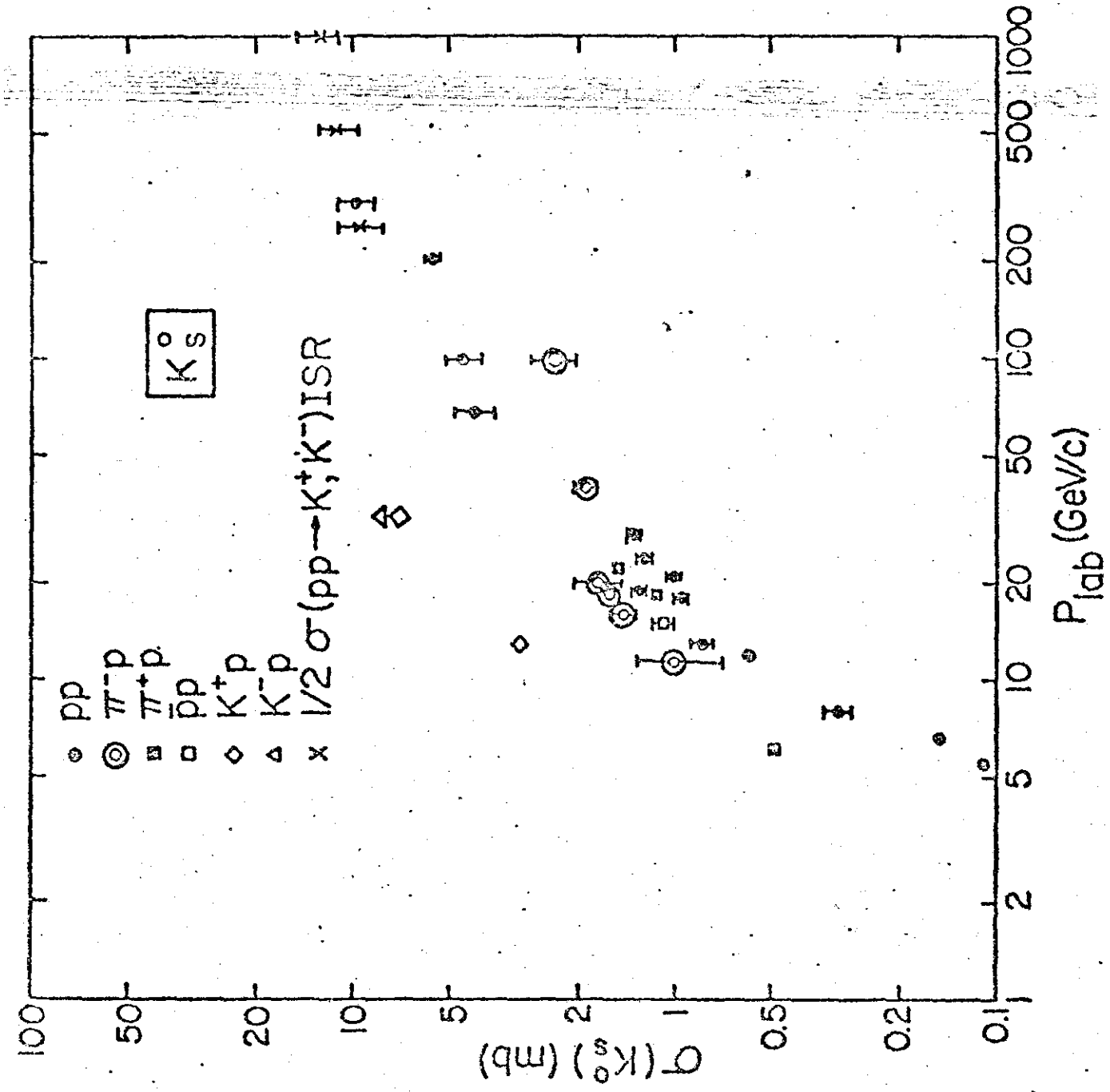
pp
π⁻p
π⁺p
p̄p
K⁺p
K⁻p
1/2 σ(pp→K⁺K⁻)ISR
K°s
σ(K°s) (mb)
P_lab (GeV/c)
100
50
20
10
5
2
1
0.5
0.2
0.1
2
5
10
20
50
100
200
500
1000

Fig. 3

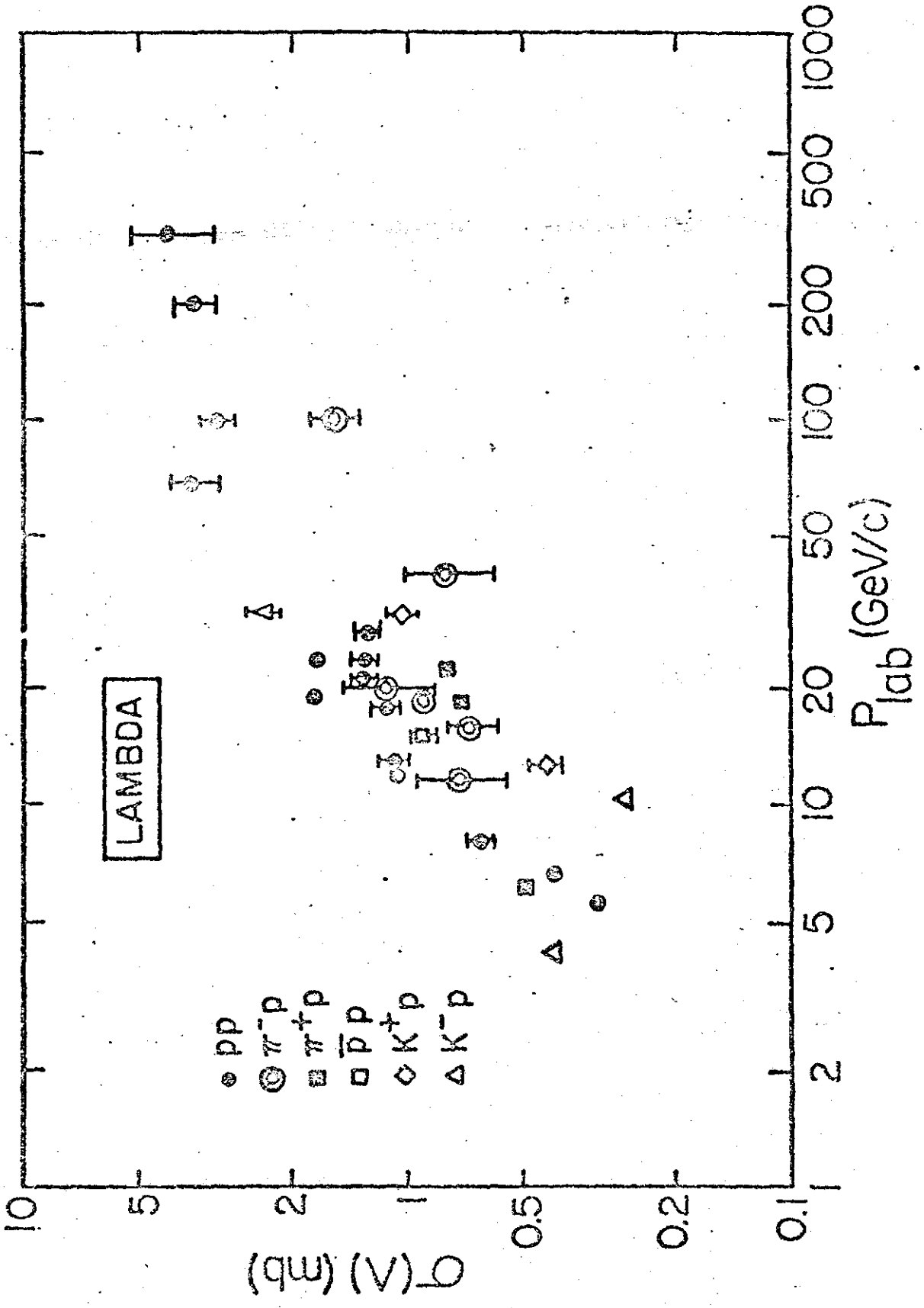
LAMBDA
pp
$\pi^- p$
$\pi^+ p$
$\bar{p} p$
$K^+ p$
$K^- p$
$\sigma(\Lambda)$ (mb)
$P_{lab}$ (GeV/c)
10
5
2
1
0.5
0.2
0.1
2
5
10
20
50
100
200
500
1000

Fig.4

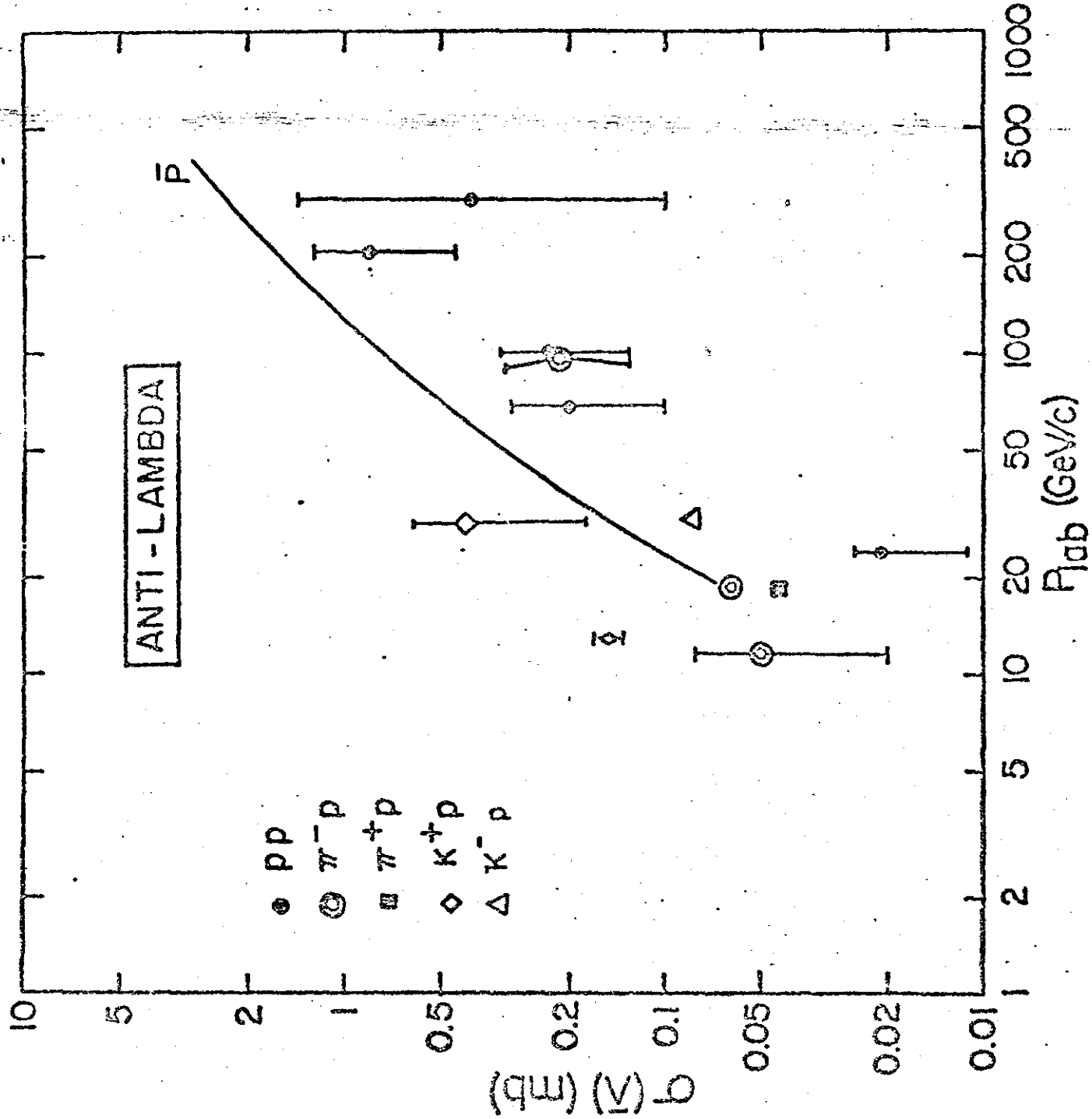
ANTI-LAMBDA
P
p p
π⁻ p
π⁺ p
K⁺ p
K⁻ p
σ (Λ̄) (mb)
10
5
2
1
0.5
0.2
0.1
0.05
0.02
0.01
1
2
5
10
20
50
100
200
500
1000
P_lab (GeV/c)

Fig. 5

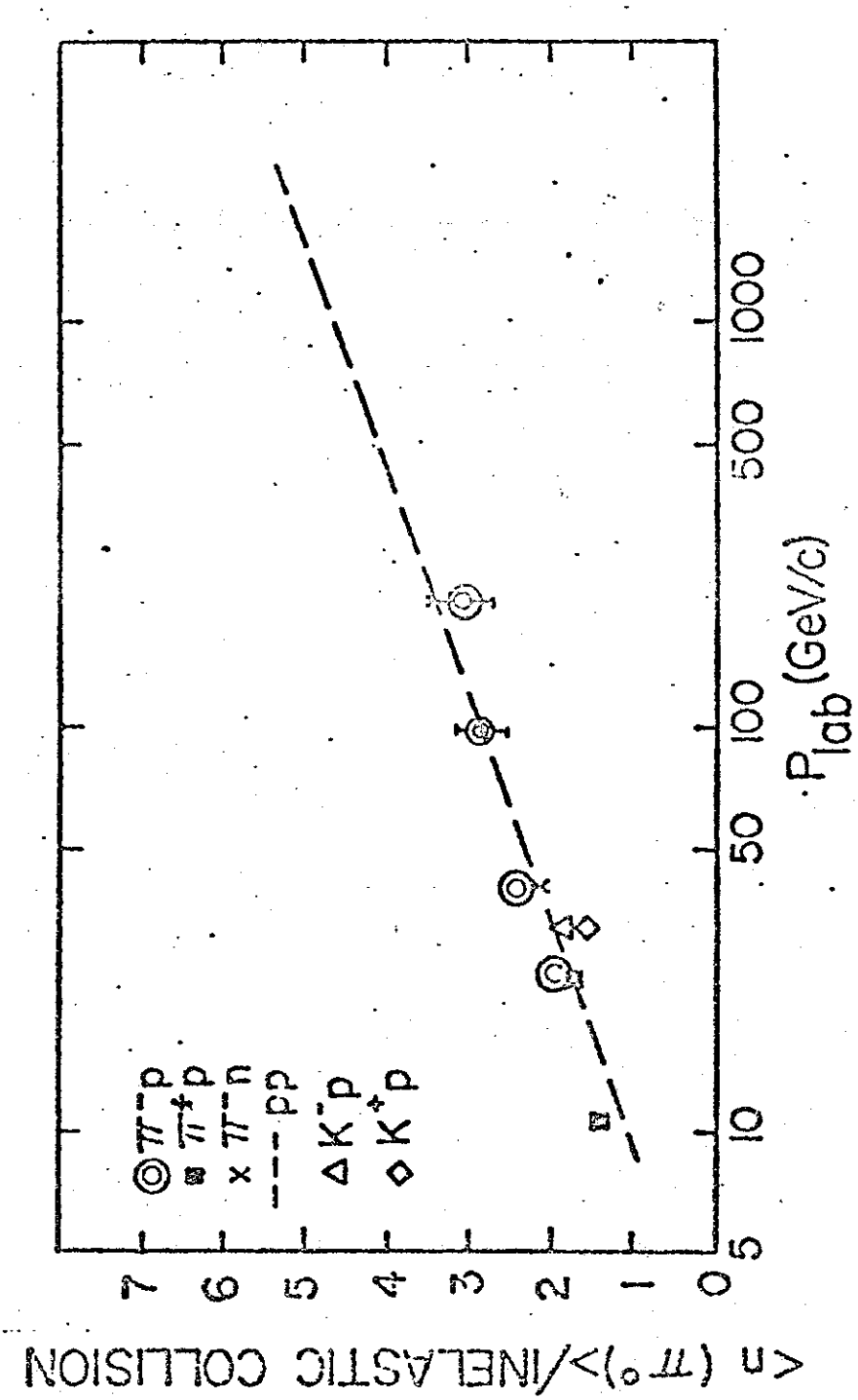
$\pi^- p$
$\pi^+ p$
$\pi^- n$
$pp$
$K^- p$
$K^+ p$
$P_{lab}$ (GeV/c)
5
10
50
100
500
1000
0
1
2
3
4
5
6
7
$\langle n(\pi^0)\rangle$/INELASTIC COLLISION

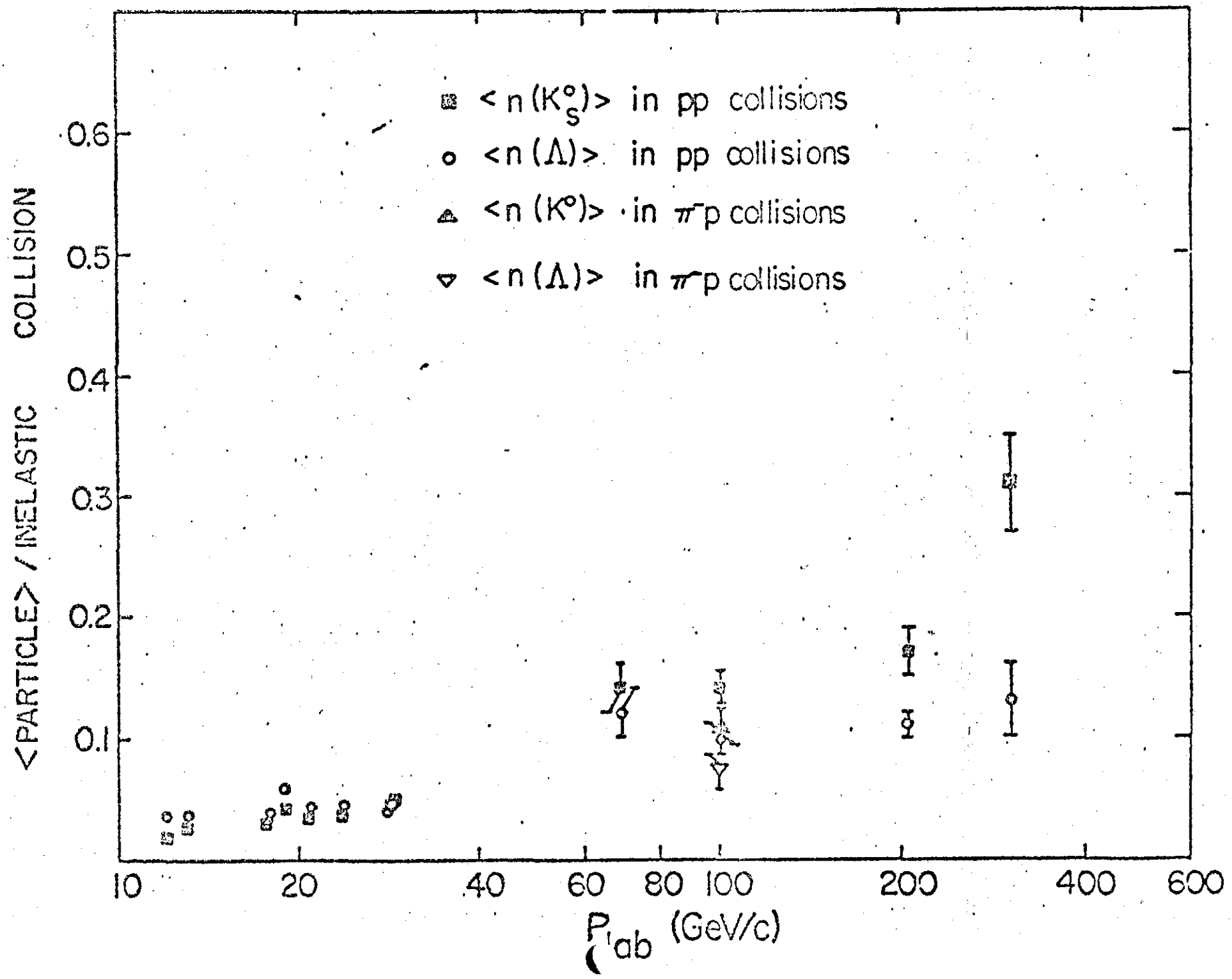
<n(K°s)> in pp collisions
<n(Λ)> in pp collisions
<n(K°)> in π⁻p collisions
<n(Λ)> in π⁻p collisions
<PARTICLE> / INELASTIC COLLISION
0.6
0.5
0.4
0.3
0.2
0.1
10
20
40
60
80
100
200
400
600
P lab (GeV/c)

Fig. 6

Fig. 7

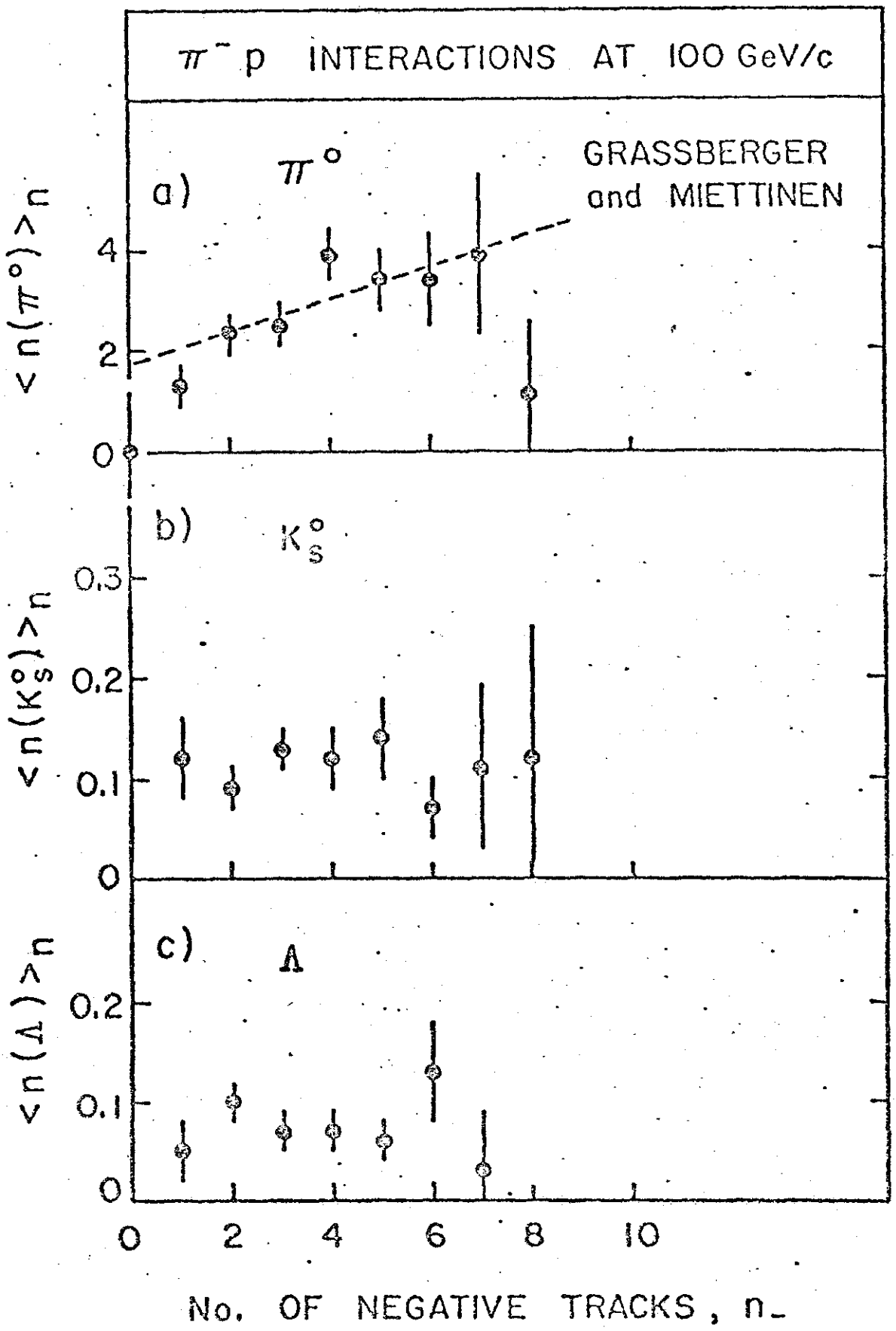
$\pi^- p$ INTERACTIONS AT 100 GeV/c
a)
$\pi^0$
GRASSBERGER and MIETTINEN
$\langle n(\pi^0) \rangle_n$
4
2
0
b)
$K_s^0$
$\langle n(K_s^0) \rangle_n$
0.3
0.2
0.1
0
c)
$\Lambda$
$\langle n(\Lambda) \rangle_n$
0.2
0.1
0
0
2
4
6
8
10
No. OF NEGATIVE TRACKS, $n_-$

Fig. 8

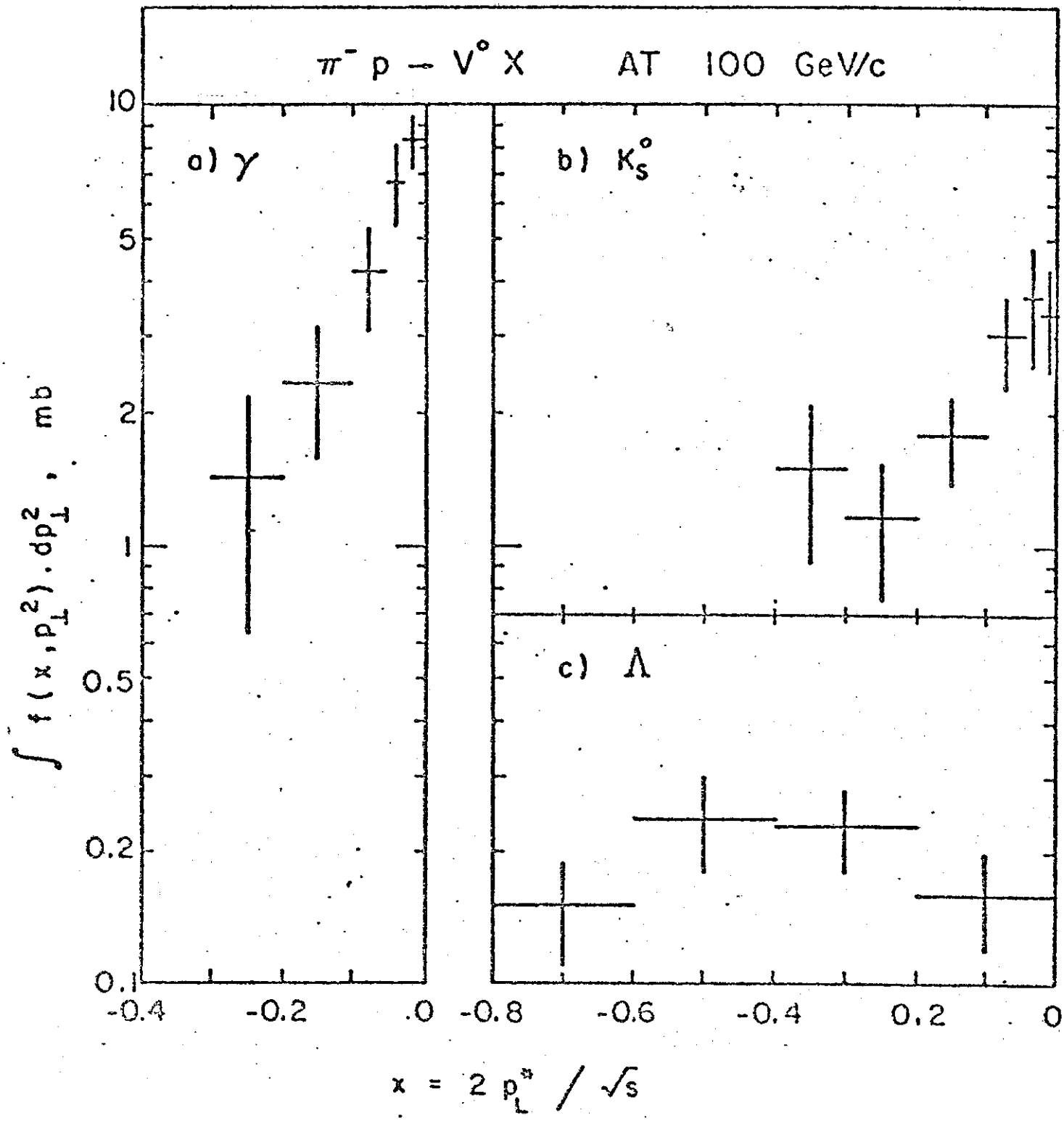
$\pi^- p \to V^\circ X$ AT 100 GeV/c
a) $\gamma$
b) $K_S^\circ$
c) $\Lambda$
$\int f(x, p_\perp^2) \cdot dp_\perp^2$ , mb
10
5
2
1
0.5
0.2
0.1
-0.4
-0.2
0
-0.8
-0.6
-0.4
0.2
0
$x = 2 p_L^* / \sqrt{s}$

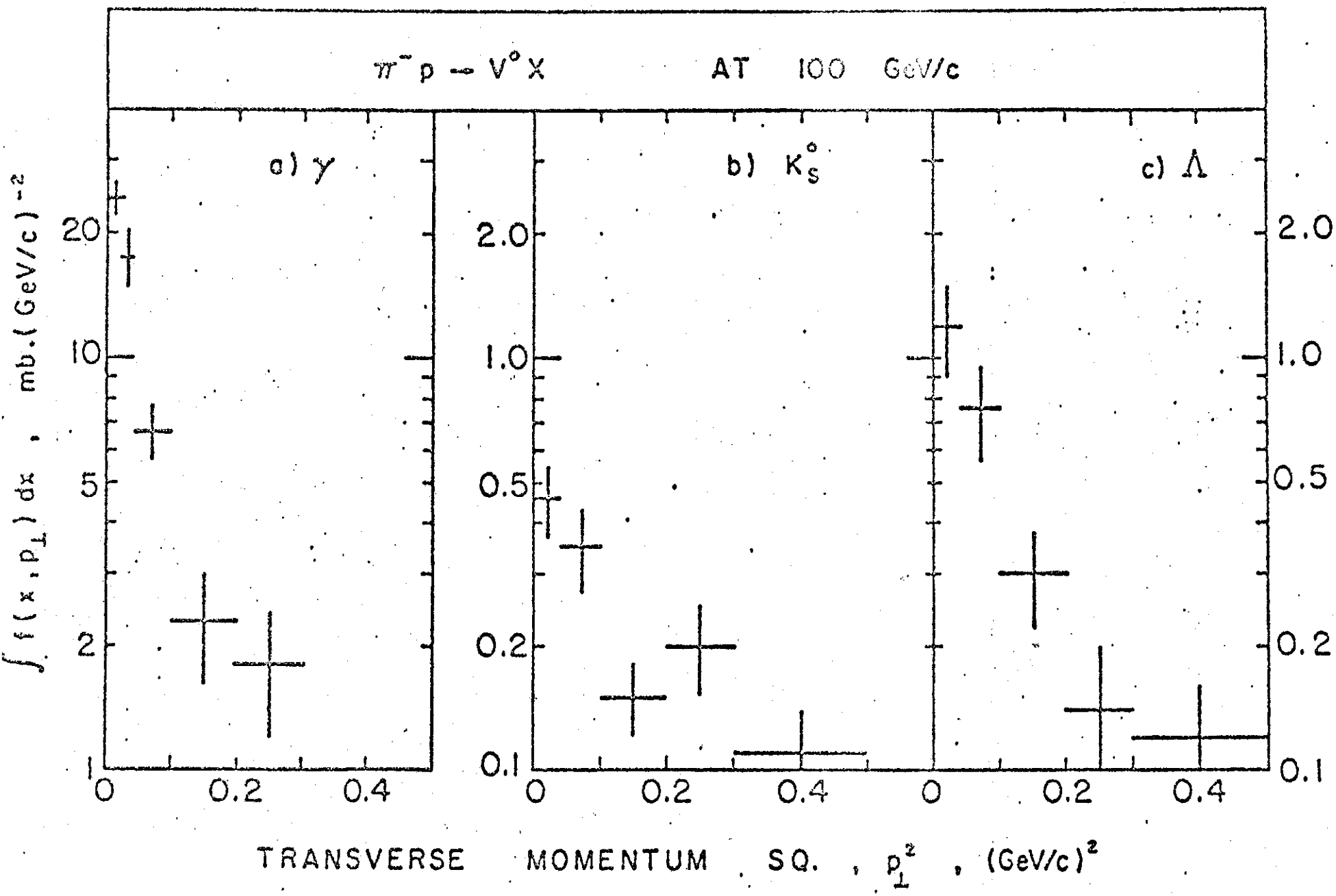
$\pi^- p \to V^\circ X$ AT 100 GeV/c
a) $\gamma$
b) $K_S^\circ$
c) $\Lambda$
$\int f(x, p_\perp)\, dx$ , mb.(GeV/c)$^{-2}$
20
10
5
2
1
2.0
1.0
0.5
0.2
0.1
0
0.2
0.4
TRANSVERSE MOMENTUM SQ. , $p_\perp^2$ , (GeV/c)$^2$

Fig. 3

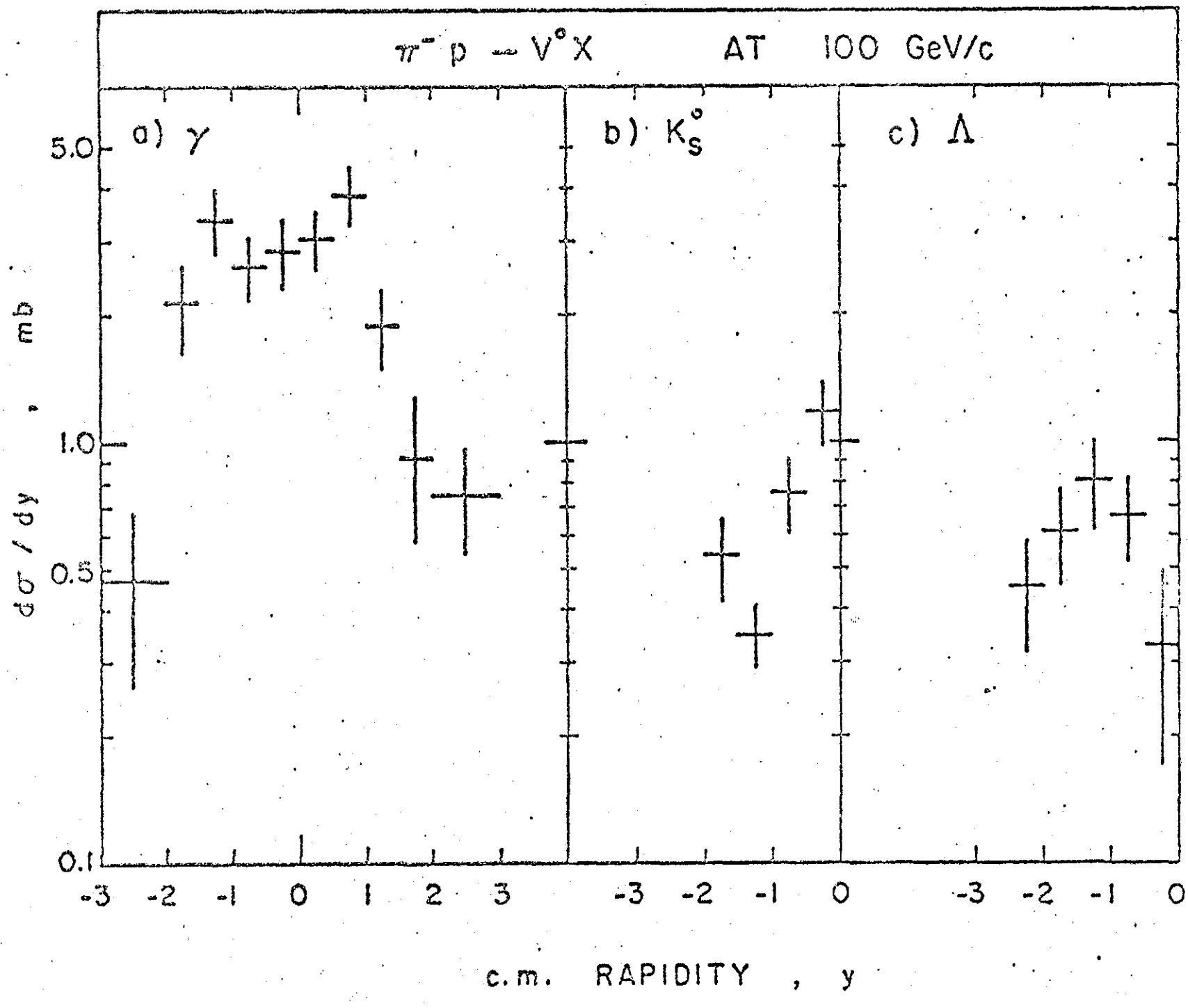
$\pi^- p \to V^\circ X$ AT 100 GeV/c
a) $\gamma$
b) $K_S^\circ$
c) $\Lambda$
5.0
1.0
0.5
0.1
$d\sigma / dy$ , mb
-3 -2 -1 0 1 2 3
-3 -2 -1 0
-3 -2 -1 0
c.m. RAPIDITY , y

Fig. 10